JOURNAL OF VIROLOGY, Sept. 1996, p. 6508–6515 Vol. 70, No. 9
0022-538X/96/$04.00+0

Transmembrane Domain of Influenza Virus Neuraminidase, a Type II Protein, Possesses an Apical Sorting Signal in Polarized MDCK Cells

A. KUNDU, R. T. AVALOS, C. M. SANDERSON, AND D. P. NAYAK*

Jonsson Comprehensive Cancer Center, Department of Microbiology and Immunology, University of California at Los Angeles, Los Angeles, California 90095-1747

Received 8 April 1996/Accepted 11 June 1996

The influenza virus neuraminidase (NA), a type II transmembrane protein, is directly transported to the apical plasma membrane in polarized MDCK cells. By using deletion mutants and chimeric constructs of influenza virus NA with the human transferrin receptor, a type II basolateral transmembrane protein, we investigated the location of the apical sorting signal of influenza virus NA. When these mutant and chimeric proteins were expressed in stably transfected polarized MDCK cells, the transmembrane domain of NA, and not the cytoplasmic tail, provided a determinant for apical targeting in polarized MDCK cells and this transmembrane signal was sufficient for sorting and transport of the ectodomain of a reporter protein (transferrin receptor) directly to the apical plasma membrane of polarized MDCK cells. In addition, by using differential detergent extraction, we demonstrated that influenza virus NA and the chimeras which were transported to the apical plasma membrane also became insoluble in Triton X-100 but soluble in octylglucoside after extraction from MDCK cells during exocytic transport. These data indicate that the transmembrane domain of NA provides the determinant(s) both for apical transport and for association with Triton X-100-insoluble lipids.

Infection of polarized epithelial cells by enveloped viruses and expression of viral envelope proteins have been extensively used as a tool to study membrane biogenesis and protein sorting. In polarized epithelial cells, enveloped viruses are known to bud asymmetrically from the cell surface (41, 43, 48, 57). Orthomyxoviruses and paramyxoviruses have been shown to bud from the apical domain of the plasma membrane, whereas vesicular stomatitis virus and retroviruses bud from the basolateral surface. Asymmetrical budding of enveloped viruses is considered to be an important determinant in virus biology, including viral pathogenesis. A Sendai virus mutant which exhibits bipolar budding in polarized epithelial cells was found to be highly pathogenic and pantropic for mice, whereas the wild-type Sendai virus exhibiting apical budding was less virulent and pneumotropic (55, 56). The budding site of enveloped viruses appears to be determined, at least partly, by the asymmetrical targeting of transmembrane viral proteins; i.e., the transmembrane viral proteins are sequestered preferentially in the same plasma membrane domain from which the virus buds. Furthermore, viral transmembrane proteins expressed individually from cloned cDNAs in the absence of other viral proteins are targeted to the same membrane domain in polarized epithelial cells as in virus-infected cells (8, 12, 16, 44, 45). Therefore, each transmembrane viral protein must possess determinants within the structure of the polypeptide backbone for either apical or basolateral sorting in polarized epithelial cells.

Despite the great interest in defining the structural determinants of apical and basolateral sorting signals and elucidating the mechanism of polarized sorting of membrane proteins in epithelial cells, little is known about the sequence or structure requirements of sorting signals or about the mechanism of the sorting process, including the components of the sorting apparatus. For basolateral proteins of either type I or II, it appears that the sorting signal(s) resides within the cytoplasmic tail (1, 3, 6, 7, 9, 13, 14, 23, 25, 26, 29, 40, 61) although neither a consensus sequence nor a specific structural element of these basolateral targeting signals has been identified but the presence of a tyrosine residue(s) and its location may provide a critical determinant(s) for basolateral targeting of some proteins (14, 22, 29, 58). However, some basolateral proteins, like the envelope protein (gp52) of spleen focus-forming virus, which does not contain a cytoplasmic tail, are transported to the basolateral surface with reduced efficiency (17). Similarly, the basolateral transport of aminopeptidase N in Caco-2 cells is also independent of a cytoplasmic tail (60).

For apical proteins, the information about the nature of the targeting sequence is even more sparse and varied (53). For apical membrane proteins which are anchored by a glycosylphosphatidylinositol (GPI) moiety and lack the cytoplasmic tail, GPI appears to provide the signal for apical targeting (24, 26, 38, 62). Furthermore, clustering of GPI-anchored proteins with Triton X-100 (T-X-100)-insoluble sphingolipid-containing vesicles appears to provide the apical targeting mechanism for these proteins. In type I transmembrane proteins, such as influenza virus hemagglutinin (HA), it appears that the ectodomain possesses a signal(s) for apical sorting (31–33, 47). We have recently shown that type II transmembrane proteins such as influenza virus neuraminidase (NA) possess two signals—one in the ectodomain and the other in the cytoplasmic tail or transmembrane domain (19, 20). In this study, we further dissected the location of the apical sorting signal of NA and found evidence that an apical sorting signal is present in the transmembrane domain and not in the cytoplasmic tail of NA. In addition, we present preliminary evidence that the transmembrane domain of NA also provides the determinants for interaction with T-X-100-insoluble lipids, as has been found for GPI-anchored proteins; this has been reported to be a critical factor for apical targeting of these proteins (24, 26, 38, 62).

* Corresponding author. Phone: (310) 825-8558. Fax: (310) 206-3865.

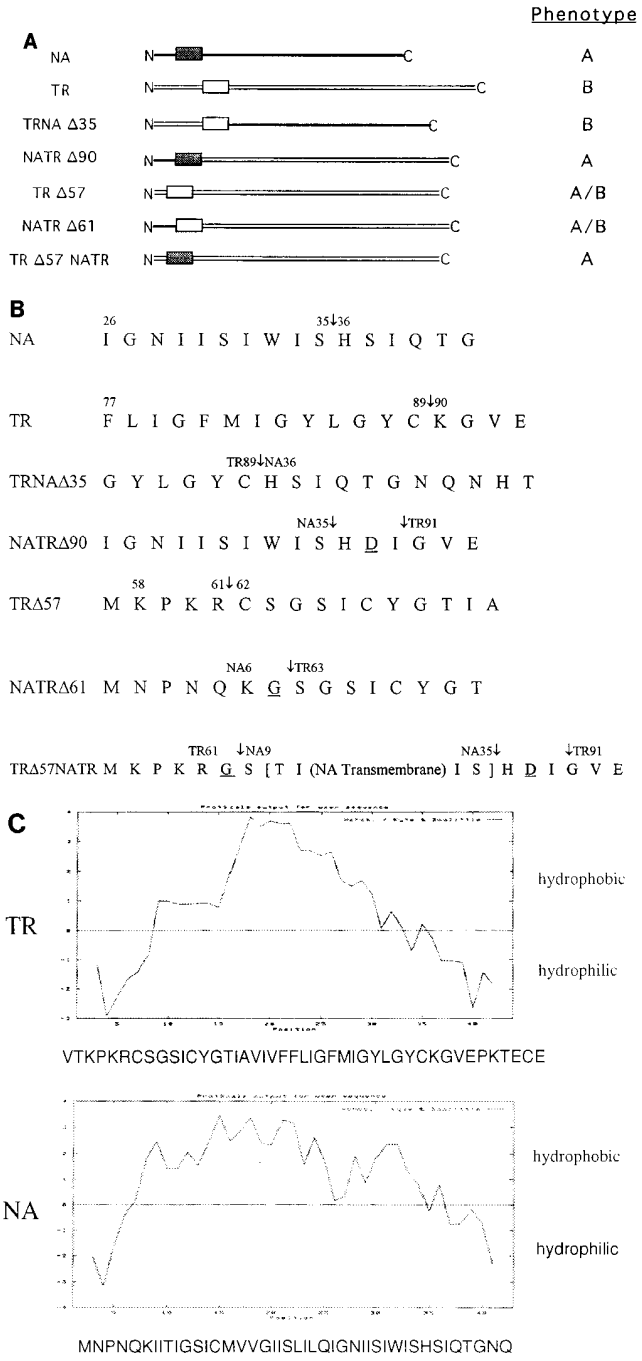

FIG. 1. Schematic representation of the primary structures of NA, TR, TRNAΔ35, NATRΔ90, TRΔ57, NATRΔ61, and TRΔ57NATR as predicted from the DNA sequences. (A) Dotted boxes and single lines represent the influenza virus NA sequence, and open boxes and double lines represent the human TR sequence. A, apical; B, basolateral. (B) The expected amino acid sequences at the junction sites of the proteins diagrammed in panel A. Vertical arrows indicate junction sequences. Extra or mutated amino acids introduced at the junction site as a result of the construction strategy are underlined. Amino acids are numbered in accordance with wild-type NA or TR. (C) Hydropathy profile and sequence comparison of the transmembrane domains of WSN NA and TR.

Construction and expression of chimeric mutants. The wild-type influenza virus and the NA and transferrin receptor (TR) chimeric and deletion mutants of influenza virus used in these experiments are shown in Fig. 1. The TRNAΔ35, NATRΔ90, and TRΔ57 sequences have been reported previously (20). TRNAΔ35 has the ectodomain of NA and the transmembrane domain and cytoplasmic tail of TR. NATRΔ90 has the ectodomain of TR but the transmembrane domain and cytoplasmic tail of NA. TRΔ57 lacks the entire cytoplasmic tail of TR except the last four amino acids. NATRΔ61 was created to swap the 6-amino-acid NA tail with the 61-amino-acid tail of TR, and it also contained the TR transmembrane domain and the TR ectodomain. For construction of NATRΔ61, a DNA segment (1,409 bp) containing the complete influenza virus (A/WSN/33) NA cDNA was isolated by *Eco*RI digestion of pGNA (2), filled in with the Klenow fragment of DNA polymerase I, and cloned into the *Sma*I site of M13mp19. An *Eco*RI site was created at the junction of the cytoplasmic tail and the transmembrane domain of NA, and the entire NA fragment containing the *Eco*RI site was cut with *Kpn*I and *Hin*dIII and subcloned into pRSETB (Invitrogen, San Diego, Calif.) to create pRSETBNA. Similarly, an *Eco*RI site was created at the junction of the cytoplasmic tail and transmembrane domain of TR in M13mp19 TR and the entire TR fragment was cloned into pGEM3 to create pGTRΔ1. pGTRΔ1 was digested completely with *Eco*RI and partially with *Hin*dIII. The fragment obtained, containing the transmembrane domain and ectodomain of TR, was cloned into *Eco*RI- and *Hin*dIII-digested pRSETBNA containing the cytoplasmic tail of NA to give plasmid pRSETBNATRΔ61. The partially *Bam*HI- and *Hin*dIII-digested DNA fragment containing the cytoplasmic tail of NA and the transmembrane domain and ectodomain of TR from pRSETBNATRΔ61 was cloned into pGEM3 to give pGNATRΔ61. Finally, *Sma*I and *Nhe*I fragments from pGNATRΔ61 were cloned into *Pvu*II and *Nhe*I sites of pMEP4 (Invitrogen).

TRΔ57NATR was created to swap the transmembrane domain of TR with that of NA. It has a 4-amino-acid TR tail, a 29-amino-acid NA transmembrane domain, and the entire TR ectodomain. For construction of TRΔ57NATR, a *Bam*HI (B) site was created at the junction of the cytoplasmic tail and transmembrane domain of both M13mp19 TRΔ57 and M13mp19 NATRΔ90 to generate M13mp19 TRΔ57B and M13mp19 NATRΔ90B, respectively. The entire TRΔ57 DNA fragment from M13mp19 TRΔ57B containing the newly created *Bam*HI site was cloned into pGEM3 to generate plasmid pGTRΔ57B. The *Bam*HI-*Sph*I fragment containing the transmembrane domain of NA and the ectodomain of TR was isolated from M13mp19 NATRΔ90B and cloned into *Bam*HI and *Sph*I sites of pGTRΔ57B, replacing the transmembrane domain and ectodomain of TR while retaining the last four amino acids of the TR cytoplasmic tail to create plasmid pGTRΔ57NATR. Finally, an *Sma*I- and *Nhe*I-digested TRΔ57NATR DNA fragment from pGTRΔ57NATR was cloned into the *Pvu*II and *Nhe*I sites of pMEP4. All plasmids were sequenced through the chimeric junctions or deletion points to confirm that the expected codons for amino acids were in phase.

Wild-type and chimeric constructs were transfected into MDCK cells with a pMEP4 expression vector, and stable hygromycin-resistant clones of cells expressing the desired proteins were obtained as described previously (20). For expression, hygromycin-resistant cells were induced with $CdCl_2$ (2 μM) and pulse-labeled for 2 h with [^{35}S]cysteine and tran[^{35}S]label and cell lysates were immunoprecipitated with appropriate antibodies. The results showed that the wild-type and mutant proteins were expressed efficiently in stable MDCK cell lines after $CdCl_2$ induction (data not shown). A lower level of the expressed protein was observed in transfected cells before induction. Next, the intracellular transport

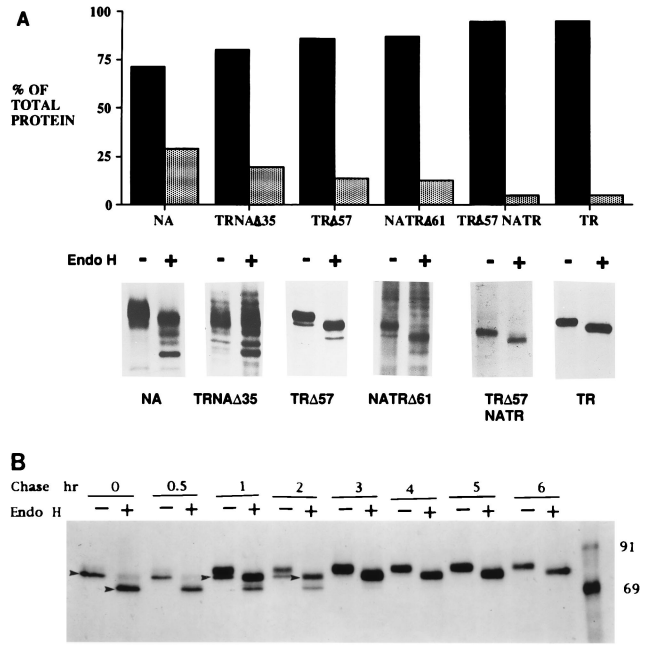

FIG. 2. Acquisition of endo H resistance by wild-type and mutant proteins. (A) Transfected MDCK cell lines were cultured for 48 h and induced with $CdCl_2$ for 16 h, labeled with 200 μCi each of [^{35}S]cysteine and [^{35}S]methionine for 90 min, and chased for 90 min. Cells were lysed and immunoprecipitated (20). The immunoprecipitates were split in half and treated with endo H (+) or mock treated (−) (19). Samples were analyzed by sodium dodecyl sulfate-polyacrylamide gel electrophoresis (21) and fluorography. The fluorographs were quantified by densitometric analysis (50). The percentages of endo H-resistant (solid bars) and -sensitive (shaded bars) proteins were calculated from the endo H-treated (+) lanes by using the fastest-migrating band as the endo H-sensitive band and the bands above this as endo H-resistant forms of the proteins. Note that for NA and TRNAΔ35, all bands above the fastest-migrating band were considered endo H resistant. For TR and constructs containing the TR ectodomain, which are efficiently transported, the completely endo H-sensitive form was hardly visible after the chase. Similar results were obtained in four independent experiments with a standard deviation of less than 10% of the mean. (B) MDCK cells expressing TRΔ57NATR were induced as described above, pulse-labeled for 20 min with 400 μCi each of [^{35}S]cysteine and [^{35}S]methionine, and chased for the times indicated above the lanes. Cells were lysed and immunoprecipitated, and one half was treated with endo H (+) and the other half was mock treated (−). The fastest-migrating band immediately after the chase in the endo H-treated (+) sample shows the position of the endo H-sensitive form; the intermediate band is partially the endo H-resistant form, as only one of the two carbohydrate moieties of TR acquires endo H resistance. The topmost band shows the position of the protein before endo H treatment. The numbers on the right are molecular sizes in thousands. The arrowheads indicate the positions of partially endo H-resistant proteins.

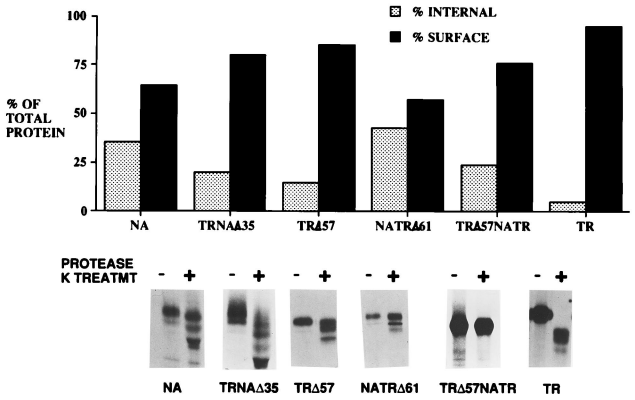

FIG. 3. Surface expression of NA, TR, TRNAΔ57, NATRΔ61, TRΔ57NATR, and TR in transfected MDCK cells. Transfected MDCK cell lines were cultured for 48 h and induced overnight with $CdCl_2$. Cells were then pulse-labeled with 200 μCi each of [^{35}S]cysteine and [^{35}S]methionine for 90 min, followed by a 90-min chase. Cells were then treated with proteinase K (0.8 mg/ml) at 4°C for 60 min (19). Mock-treated (−) and proteinase K-treated (+) cells were then lysed with radioimmunoprecipitation assay buffer. Lysates were clarified, immunoprecipitated, and analyzed by sodium dodecyl sulfate-polyacrylamide gel electrophoresis. Autoradiograms were quantified by densitometry as described previously (19, 20). One-fifth of the total (*T*) samples and all of the proteinase K-treated samples were analyzed by polyacrylamide gel electrophoresis. For quantification, values were normalized. Proteinase K-treated samples represented the internal (*I*) protein, and the cell surface (*S*) protein as a percentage of the total protein was calculated as follows: $S = \{[(T \times 5) - I]/(T \times 5)]\} \times 100$. Similar results were obtained in three independent experiments with a standard deviation of less than 9% of the mean.

and cell surface expression of the wild-type and chimeric proteins were determined as reported previously (19, 20). Accordingly, we examined each protein for endonuclease H (endo H) resistance, which indicates the acquisition of complex carbohydrates and transport through the medial Golgi during intracellular transport through the exocytic pathway. The pattern of endo H resistance depends on the nature of the ectodomain. For example, WSN NA has four potential N-linked glycosylations and exhibits heterogeneous endo H resistance in both virus-infected cells (11) and cells expressing NA from cloned cDNA (19). On the other hand, the TR ectodomain possesses two N-linked carbohydrates, only one of which acquires endo H resistance. To determine the endo H resistance pattern of the expressed proteins, MDCK cell lines were induced, labeled for 90 min, and chased for 90 min. Cell lysates were then immunoprecipitated and treated with endo H. The results obtained (Fig. 2A) show that NA and TRNAΔ35, both containing the NA ectodomain, exhibited complex heterogeneous endo H resistance patterns. The fastest-migrating band after endo H treatment (+) indicates the position of the completely endo H-sensitive protein (11). Densitometric analysis showed that approximately 70 to 80% of both NA and TRNAΔ35 became partially endo H resistant. Proteins which possessed the TR ectodomain (TR, TRΔ57, NATRΔ61, and TRΔ57NATR) all exhibited similar levels of endo H resistance, and over 85% of the protein became partially endo H resistant.

We further analyzed the kinetics by which TRΔ57NATR, possessing the NA transmembrane domain and the TR ectodomain, acquires endo H resistance. Induced cells expressing the chimeric protein were pulse-labeled for 20 min and chased for various times before being lysed for immunoprecipitation. The results obtained (Fig. 2B) show that TRΔ57NATR became partially endo H resistant less than 1 h into the chase, indicating that the chimera was transported efficiently through the exocytic pathway. The kinetics of TRΔ57NATR was essentially same as that of the wild-type TR reported previously (19). These results show that mutant proteins exhibit transport behavior similar to that of the wild-type proteins through the exocytic pathway.

Next we determined the amount of the wild-type and chimeric proteins present on the cell surface. Accordingly, cells expressing different chimeric and wild-type proteins were labeled for 90 min and chased for 90 min. Parallel dishes were either mock treated or treated with proteinase K (19). We and others have previously determined that proteinase K treatment removes all cell surface protein, leaving only the internal proteins, and the mock-treated cells represent the total (internal and cell surface) protein (19, 27). The amount of cell surface protein was determined by subtraction of the internal (proteinase K-treated) protein from the total protein. The results obtained (Fig. 3) show that most of the protein (>65%) was present on the cell surface. Similar results were obtained after

surface biotinylation (data not shown), provided that the biotinylation data were appropriately corrected since surface biotinylation measures only 20 to 30% of the surface protein (19, 23, 27). Taken together, these results show that the deletion mutants and chimeras tested exhibit transport behavior through the exocytic pathway to the cell surface similar to that of the wild-type proteins.

NA tail does not possess an apical sorting signal. Since in most basolateral proteins, including TR, cytoplasmic tails have been shown to possess the sorting signal for basolateral transport (3, 7, 9, 13, 14, 23, 37, 39, 40), we wanted to determine if the cytoplasmic tail of NA also possesses an apical sorting signal. We have previously shown that tail-free TR (TRΔ57, possessing only 4 of the 61 amino acids of the cytoplasmic tail) lacks a sorting signal (20). The protein was missorted, i.e., present equally in both apical and basolateral plasma membranes (Fig. 4A, column 3). TRΔ57 also lacks the sequence required for endocytosis, which is present in amino acid residues 19 to 28 with tyrosine at position 20 (15). We therefore created NATRΔ61 (Fig. 1), in which the four amino acids present in the cytoplasmic tail of TRΔ57 were swapped with the six amino acids which constitute the entire cytoplasmic tail of NA. Polarized MDCK cells expressing NATRΔ61 were labeled for 90 min and chased for 90 min, and the expression of proteins on the apical and basolateral surfaces of parallel cultures was analyzed by biotinylation and immunoprecipitation as reported previously (20). The results obtained show that NATRΔ61 containing the cytoplasmic tail of NA when expressed in polarized MDCK cells was also missorted (Fig. 4A, column 4) and present, like TRΔ57 (Fig. 4A, column 3), equally on both apical and basolateral plasma membranes, implying that the NA tail, unlike the cytoplasmic tail of basolateral proteins, does not provide the determinants for apical sorting in polarized MDCK cells.

NA transmembrane domain possesses an apical sorting signal. Since the NA tail does not possess an apical sorting signal, we wanted to determine whether the NA transmembrane domain provides the determinant for apical sorting or both the transmembrane domain and cytoplasmic tail function cooperatively in apical sorting. Accordingly, we swapped the transmembrane domain of TRΔ57 with that of NA to create TRΔ57NATR (Fig. 1). Polarized MDCK cells expressing TRΔ57NATR were labeled and analyzed for domain-specific expression by biotinylation (20). The results obtained show that TRΔ57NATR (Fig. 4A, column 5), unlike TRΔ57, was sorted apically in polarized MDCK cells, implying that the transmembrane domain of NA possesses an apical sorting signal. The level of apical-basolateral membrane expression of TRΔ57NATR was essentially the same as that of the wild-type NA or NATRΔ90 (20), possessing both the transmembrane domain and cytoplasmic tail of NA attached to the ectodomain of TR. These results obtained with a TRΔ57NATR chimeric protein were surprising, since the transmembrane polypeptide domain has not been implicated in either apical or basolateral membrane sorting. We confirmed these results by using multiple clones, as well as uncloned hygromycin-resistant MDCK cells transfected with TRΔ57NATR cDNA.

We have previously reported that NA and NATRΔ90 are directly transported to the apical plasma membrane, whereas TR and TRNAΔ35 are directly targeted to the basolateral membrane (20). To determine if TRΔ57NATR is sorted directly to the apical surface in MDCK cells or if the protein reaches first the basolateral surface and then the apical surface by transcytosis, we did pulse-chase experiments and determined the kinetics of appearance of the protein at the apical and basolateral surfaces. The results obtained (Fig. 4B) show that TRΔ57NATR, containing the transmembrane domain of NA, was first detected on the apical plasma membrane and reached a maximum by 60 min of the chase. A small amount of protein reached the basolateral surface with a peak at 2 h of the chase. However, at no time during the chase did the amount of the protein at the basolateral surface exceed that present on the apical surface. Similar results were obtained in another, independent experiment. These results and the kinetics of apical transport are similar to those of NATRΔ90, which we have reported previously (20). NATRΔ90 contains both the cytoplasmic and transmembrane domains of NA attached to the ectodomain of TR. We conclude from these results that TRΔ57NATR, containing only the transmembrane domain of NA, was targeted directly to the apical surface and not by transcytosis via the basolateral surface. This conclusion is further supported by the fact that TRΔ57NATR lacks the endocytic signal present in its cytoplasmic tail (15) and that endocytosis is required for transcytosis of any protein. For the same reason, we think that slow accumulation of the small amount of TRΔ57NATR at the basolateral surface is due not to transyctosis from the apical to the basolateral surface but to partial missorting, as has been observed for most apical proteins.

Association of the apical proteins with T-X-100-insoluble lipids. Since GPI-linked proteins are sorted apically (24, 26, 38, 62) and have been shown to associate with T-X-100-insoluble lipids (5, 49), we wanted to determine if the transmembrane type II proteins which are sorted apically also associate with T-X-100-insoluble lipids. Accordingly, cells expressing apical, basolateral, or missorted proteins were labeled for 90 min, chased for 90 min, and extracted with T-X-100 as reported previously (49). The results obtained (Fig. 5A) show that basolateral proteins like TR and TRNAΔ35 and missorted proteins TRΔ57 and NATRΔ61 were predominantly (70 to 95%) T-X-100 soluble after the chase, whereas significant fractions (60 to 85%) of apical proteins like NA, NATRΔ90, and TRΔ57NATR (Fig. 5A) were insoluble after T-X-100 extraction of MDCK cells expressing these proteins. In addition, other apical proteins, like influenza virus HA (Fig. 5A) and GPI-linked human alkaline placental phosphatase (5), were also 50 to 60% T-X-100 insoluble (data not shown). Previously published data also show that influenza virus HA (54), Sendai virus F and HN in virus-infected cells (49), and GPI-linked GDI-DAF (62) were approximately 50% insoluble when subjected to T-X-100 extraction under similar conditions. These results show that all of the apical proteins exhibited higher levels of T-X-100 insolubility than either basolateral or missorted proteins.

To determine if the T-X-100 insolubility was due to the association of these proteins with the cytoskeleton or with the T-X-100-insoluble lipids, cells expressing apical proteins which exhibited resistance to T-X-100 extraction were extracted with octylglucoside (OG), which has been shown to dissolve T-X-100-insoluble lipids (5). The results obtained show that all of these apical proteins were rendered completely soluble by OG extraction (Fig. 5B). Similarly, Sendai virus F and HN (49) and influenza virus HA in influenza virus-infected cells were also soluble in OG (Fig. 5B). On the other hand, the Sendai virus M and NP proteins (49), as well as the influenza virus NP and M1 proteins (unpublished data), which appear to interact with cytoskeletal components, did not become soluble after either T-X-100 or OG treatment. These results, taken together, indicate that apical type II proteins containing the NA transmembrane domain interacted with T-X-100-insoluble lipids during exocytic transport.

Conclusion. The results reported here show that the transmembrane domain of influenza virus NA, a type II integral

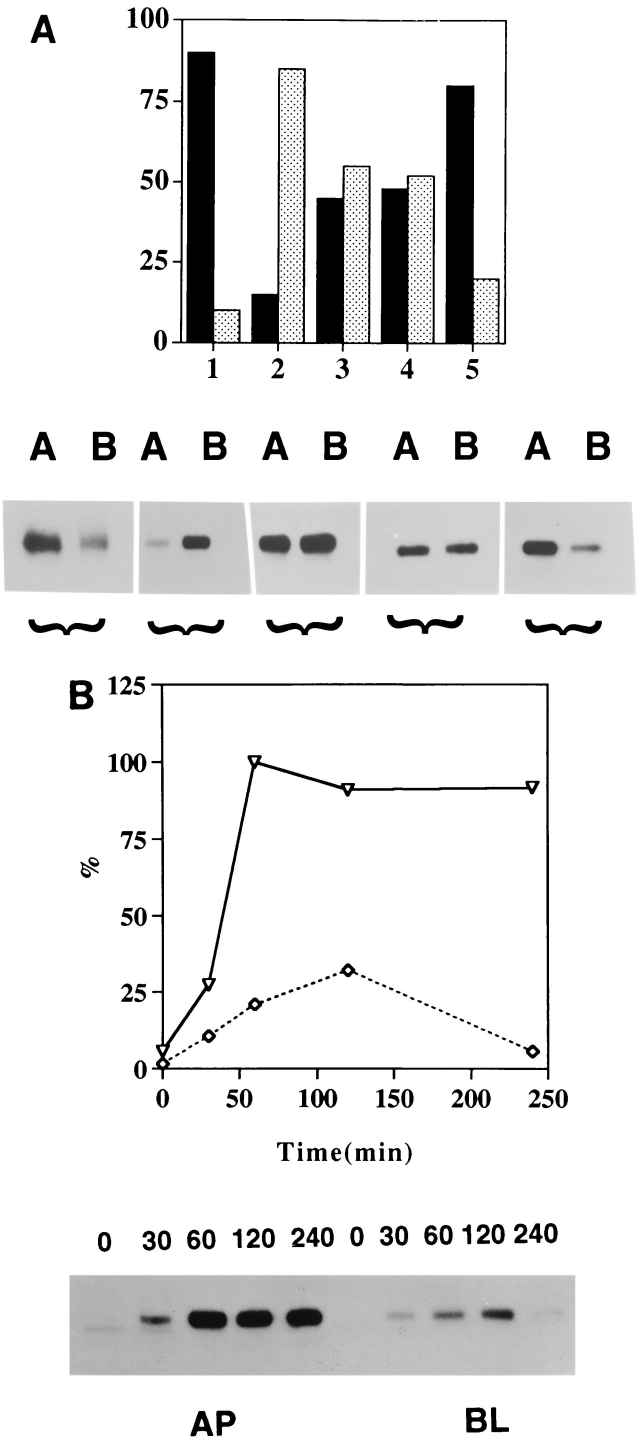

FIG. 4. Polarized surface distribution of NA, TR, TRΔ57, NATRΔ61, and TRΔ57NATR. (A) Confluent monolayers of MDCK cells were grown on filters for 5 days, pulse-labeled for 90 min with 500 μCi each of [^{35}S]cysteine and tran[^{35}S]label, and chased for 90 min. The apical (lanes A) or basolateral (lanes B) surface proteins were biotinylated (20, 42), isolated by using specific antibodies, and analyzed by sodium dodecyl sulfate-polyacrylamide gel electrophoresis and fluorography (20). The same fluorogram was quantified, and results are presented as percent apical (black bars) and percent basolateral (gray bars). Bars: 1, NA; 2, TR; 3, TRΔ57; 4, NATRΔ61; 5, TRΔ57NATR. Similar results were obtained from three independent experiments with a standard deviation of less than 10% of the mean. (B) MDCK cells expressing TRΔ57NATR were grown on filters for 5 days. The cells were labeled for 20 min with 500 μCi each of [^{35}S]cysteine and tran[^{35}S]label and chased for the times indicated above the lanes in minutes. The apical (AP) or basolateral (BL) surface proteins were biotinylated and isolated (20). Samples were analyzed by sodium dodecyl sulfate-polyacrylamide gel electrophoresis and processed for fluorography. The same fluorogram was quantified, and the results are expressed as percentages of the level of protein expression at the time of maximal expression at the cell surface (23). Symbols: ▽, apical; ◇, basolateral. Similar results were obtained from two independent experiments with a standard deviation of less than 15% of the mean.

membrane protein, possesses a signal(s) for apical sorting and can direct the ectodomain of a reporter protein, human TR, to the apical plasma membrane of polarized MDCK cells. This conclusion is based upon the observation that TRΔ57, a TR mutant lacking the first 57 of the 61 amino acids in the cytoplasmic tail, was missorted to both apical and basolateral surfaces in MDCK cells, whereas the same protein containing the transmembrane domain of NA was targeted to the apical plasma membrane. The precise reason why TRΔ57 was missorted to both apical and basolateral surfaces is open to interpretation. Since the cytoplasmic tail of TR contains the basolateral signal (20) and since this tail is missing in TRΔ57, we prefer to think that the protein lacking a specific sorting signal was transported randomly by default and not targeted to a specific plasma membrane domain (28). However, other explanations, such as that TRΔ57 possesses both apical and basolateral signals that are equal in strength and therefore the protein is targeted to both surfaces equally, although unlikely, cannot be ruled out. Irrespective of the interpretation of the reason for missorting of TRΔ57, it is obvious that when the transmembrane domain of TRΔ57 was swapped with that of NA, the TRΔ57NATR protein was directed predominantly to the apical plasma membrane in MDCK cells, demonstrating that the transmembrane domain of NA provides the determinant(s) for apical sorting of the TR ectodomain in this chimeric protein. Furthermore, since both TRΔ57 and NATRΔ61 were missorted equally to apical and basolateral surfaces, whereas TRΔ57NATR was transported to the apical surface, it is unlikely that TRΔ57NATR was apically transported by default. The pulse-chase data also show that TRΔ57NATR was directly delivered to the apical plasma membrane and that the protein was not delivered first to the basolateral membrane and then to the apical membrane by transcytosis.

Previous studies have shown that type I, as well as type II, apical proteins possess signals for polarized sorting in the ectodomain (8, 10, 20, 31–33, 47, 53). However, since the ectodomain contains the complex structural constraints required for oligomerization, intracellular transport, antigenic epitopes, glycosylation, disulfide linkages (both intramolecular and intermolecular), and other structural and functional constraints, it has not been possible to further define the ectodomain apical signal by mutational analysis or chimeric construction by using a reporter protein. Mutations or chimeric construction involving ectodomain often renders the protein defective both functionally and structurally. For GPI-anchored apical proteins lacking a cytoplasmic tail, GPI has been shown to provide the apical sorting signal (4, 5, 24, 26, 38, 61). On the other hand, most basolateral proteins of either type I or II orientation have been shown to possess a basolateral targeting signal(s) in the cytoplasmic tail (1, 3, 7, 9, 13, 14, 20, 23, 29, 37, 39, 40, 61). This basolateral signal(s) often overlaps or is found to be colinear with the signals for endocytosis (1, 3, 7, 13, 14, 18, 23, 29, 30, 35, 46). The results reported here that we obtained with NATRΔ61 show that the cytoplasmic tail of NA, unlike those of basolateral proteins, does not possess an apical sorting signal. It has been recently reported that for some secretory proteins, glycosylation provides a determinant for

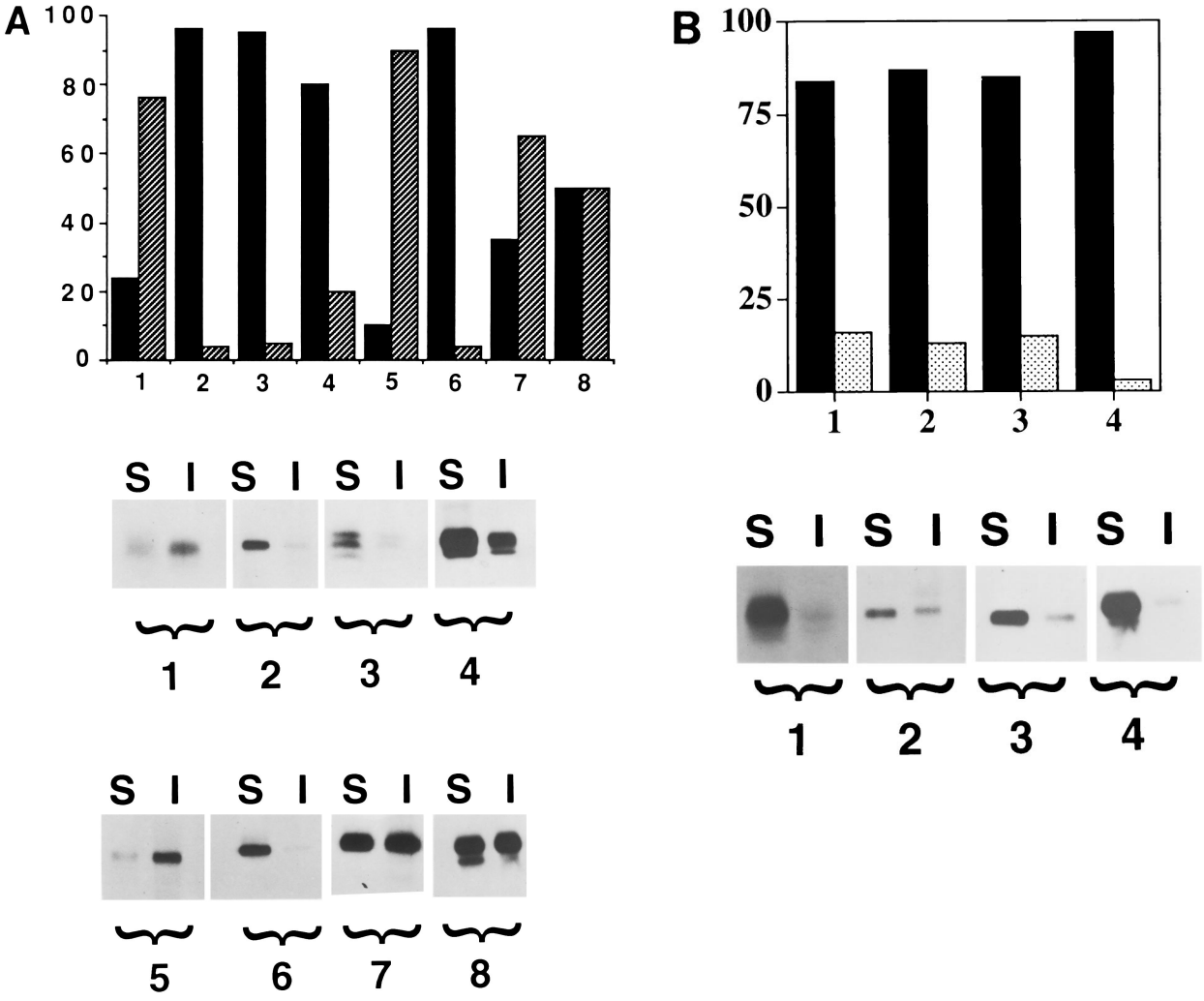

FIG. 5. T-X-100 and OG solubility of wild-type and chimeric proteins and influenza virus HA. (A) Transfected MDCK cells were grown, pulse-labeled for 90 min with 500 μCi each of [^{35}S]cysteine and tran[^{35}S]label, and then chased for 90 min in the presence of unlabeled cysteine and methionine. For influenza virus HA, MDCK cells were infected with A/WSN/33 at a multiplicity of infection of 5 (36), pulse-labeled for 10 min at 6 h postinfection with 100 μCi each of [^{35}S]cysteine and tran[^{35}S]label, and chased for 90 min. The cells were extracted with 1% T-X-100 (34, 49). Parallel dishes were used for the total, T-X-100-soluble (S), and T-X-100-insoluble (I) fractions. Each sample was immunoprecipitated with specific antibodies and analyzed by sodium dodecyl sulfate-polyacrylamide gel electrophoresis and fluorography as described previously (49). The same fluorograms were quantified for T-X-100-soluble (black bars) and T-X-100-insoluble (slash bars) proteins. Similar results were obtained in three independent experiments with a standard deviation of less than 8% of the mean. Bars: 1, NA; 2, TR; 3, TRNAΔ35; 4, TRΔ57; 5, NATRΔ90; 6, NATRΔ61; 7, TRΔ57NATR; 8, influenza virus HA. (B) MDCK cells expressing NA, NATRΔ90, and TRΔ57NATR, as well as influenza virus-infected cells, were pulse-labeled and chased as described above. The cells were then extracted with OG, and soluble (S) and insoluble (I) fractions were separated and analyzed by sodium dodecyl sulfate-polyacrylamide gel electrophoresis and fluorography. The same fluorograms were quantified, and the results are expressed as percent soluble (black bars) and percent insoluble (gray bars) for each protein. Bars: 1, NA; 2, NATRΔ90; 3, TRΔ57NATR; 4, influenza virus HA. Similar results were obtained from three independent experiments with a standard deviation of less than 10% of the mean. Recovery of the total protein in T-X-100-soluble and -insoluble proteins varied from 85 to 95%.

apical sorting (51). However, it is unlikely that glycosylation of the ectodomain plays a major role in apical transport of TRΔ57NATR, since all of the proteins containing the TR ectodomain exhibited similar glycosylation patterns and levels of endo H resistance. However, the role of glycosylation cannot be ruled out completely unless the sorting behavior of nonglycosylated proteins is determined.

The transmembrane apical sorting signal for a type II protein reported here is a novel finding, since the transmembrane peptide has not been implicated in apical sorting but the transmembrane domain of aminopeptidase N has been shown to be involved in transcytosis from basolateral to apical surfaces in Caco-2 cells (60). However, unlike aminopeptidase N, transcytosis is not involved in apical sorting of influenza virus NA. The unique feature of the transmembrane domain of NA, which either facilitates or directs apical sorting, compared with that of TR is not obvious. Both transmembrane domains are long and hydrophobic (Fig. 1C).

Our results also show that wild-type NA, as well as all apical chimeric proteins containing the transmembrane domain of NA, exhibited a higher resistance to T-X-100 detergent extraction than did either basolateral or missorted proteins (Fig. 5A) but became soluble in OG (Fig. 5B). These data support the notion that the transmembrane domain of the NA also provides determinants for T-X-100 insolubility. Similar T-X-100 insolubility has been observed in virus-infected cells for apical type I proteins like influenza virus HA (49) and Sendai virus F and HN (49). These results suggest that like GPI, the trans-

membrane domain of some apical proteins could form clusters or aggregates with T-X-100-insoluble glycosphingolipids, which have been shown to be an important component of apical sorting vesicles (52, 59). The data presented here support the model proposed for an apical sorting microdomain of the trans-Golgi network involving both a sphingolipid cluster and a cytosolic protein coat by Simons and van Meer (52). The transmembrane domain of apical proteins would facilitate binding to glycosphingolipid clusters. However, in addition, transmembrane apical proteins, unlike GPI-anchored proteins, possess cytoplasmic tails of various lengths which may interact with other components of the sorting machinery and thus may play an important role in apical sorting (28, 52, 59, 62). However, the six amino acids of NA or the four amino acids of TRΔ57NATR did not affect targeting. On the other hand, the long cytoplasmic tail of TR provides a strong basolateral signal compared with the apical signals of NA since the chimera containing the ectodomain and transmembrane domain of NA and the cytoplasmic tail of TR was targeted to the basolateral domain and exhibited T-X-100 solubility (data not shown). Further work is needed to define the relative strength of targeting signals and their interaction with lipid and protein components of the sorting apparatus. Furthermore, since some apical transmembrane proteins like Gp114 and Gp135 do not exhibit T-X-100 insolubility (62), it appears that only those apical transmembrane proteins which, like influenza virus NA, possess sorting signals both in the ectodomain and in the transmembrane domain or in the transmembrane domain would exhibit T-X-100 insolubility. On the other hand, apical proteins like Gp114 or Gp135 may possess apical signals only in the ectodomain but not in the transmembrane domain and thus may not exhibit T-X-100 insolubility (62). This implies the existence of more than one type of apical sorting machinery or different modes of interaction with the same sorting machinery.

In conclusion, we have shown that the transmembrane domain of influenza virus NA possesses an apical targeting signal and that the transmembrane domain of NA and, possibly, other type I and II proteins may facilitate interaction with T-X-100-insoluble glycosphingolipids and thus aid in apical sorting of these proteins. Further analysis of the transmembrane domain of NA and other apical domain signals would help in defining the structure and function of the apical domain signal(s) and its interaction with the sorting machinery.

We thank Eleanor Berlin and Marcia Trylch for typing the manuscript. Stable MDCK cells expressing GPI-linked human alkaline placental phosphatase were kindly provided by Deborah Brown (5).

The work reported here was supported by a Public Health Service grant from the National Institute of Allergy and Infections Diseases (AI-16348).

REFERENCES

1. **Apodaca, G., L. A. Katz, and K. E. Mostov.** 1994. Receptor-mediated transcytosis of IgA in MDCK cells is via apical recycling endosomes. J. Cell Biol. **125:**67–86.
2. **Bos, T. J., A. R. Davis, and D. P. Nayak.** 1984. NH_2 terminal hydrophobic region of influenza virus neuraminidase provides the signal function in translocation. Proc. Natl. Acad. Sci. USA **81:**2327–2331.
3. **Brewer, C. B., and M. G. Roth.** 1991. A single amino acid change in the cytoplasmic domain alters the polarized delivery of influenza virus hemagglutinin. J. Cell Biol. **114:**413–421.
4. **Brown, D. A., B. Crise, and J. K. Rose.** 1989. Mechanism of membrane anchoring affects polarized expression of two proteins in MDCK cells. Science **245:**1499–1501.
5. **Brown, D. A., and J. K. Rose.** 1992. Sorting of GPI-anchored proteins to glycolipid-enriched membrane subdomains during transport to the apical cell surface. Cell **68:**533–544.
6. **Caplan, M. J., H. C. Anderson, G. E. Palade, and J. D. Jamieson.** 1986. Intracellular sorting and polarized cell surface delivery of Na^+, K^+-ATPase, an endogenous component of MDCK cell basolateral plasma membranes. Cell **46:**623–631.
7. **Casanova, J. E., G. Apodaca, and K. E. Mostov.** 1991. An autonomous signal for basolateral sorting in the cytoplasmic domain of the polymeric immunoglobulin receptor. Cell **65:**65–75.
8. **Compton, T., I. E. Ivanov, T. Gottlieb, M. Rindler, M. Adesnik, and D. D. Sabatini.** 1989. A sorting signal for the basolateral delivery of the vesicular stomatitis virus (VSV) G protein lies in its luminal domain: analysis of the targeting of VSV G-influenza hemagglutinin chimeras. Proc. Natl. Acad. Sci. USA **86:**4112–4116.
9. **Geffen, I., C. Fuhrer, B. Leitinger, M. Weiss, K. Huggerl, G. Griffiths, and M. Speiss.** 1993. Related signals for endocytosis and basolateral sorting of the asialoglycoprotein receptor. J. Biol. Chem. **268:**20772–20777.
10. **Gottardi, C. J., and M. J. Caplan.** 1993. An ion transporting ATPase encodes multiple apical localization signals. J. Cell Biol. **121:**283–293.
11. **Hogue, B., and D. P. Nayak.** 1992. Synthesis and processing of the influenza virus neuraminidase, a type II transmembrane glycoprotein. Virology **188:** 510–517.
12. **Hughey, P. G., R. W. Compans, S. I. Zebedee, and R. A. Lamb.** 1992. Expression of the influenza A virus M2 protein is restricted to apical surfaces of polarized epithelial cells. J. Virol. **66:**5542–5552.
13. **Hunziker, W., C. Harter, K. Matter, and I. Mellman.** 1991. Basal lateral sorting in MDCK cells requires a distinct cytoplasmic domain determinant. Cell **66:**907–920.
14. **Hunziker, W., and I. Mellman.** 1989. Expression of macrophage-lymphocyte Fc receptors in Madin-Darby canine kidney cells: polarity and transcytosis differ for isoforms with or without coated pit localization domains. J. Cell Biol. **109:**3291–3302.
15. **Jing, S., T. Spencer, K. Miller, C. Hopkins, and I. S. Trowbridge.** 1990. The role of human transferrin receptor cytoplasmic domain in endocytosis: localization of a specific signal sequence for internalization. J. Cell Biol. **110:** 283–294.
16. **Jones, L. V., R. W. Compans, A. R. Davis, T. J. Bos, and D. P. Nayak.** 1985. Surface expression of influenza virus neuraminidase, an amino-terminally anchored viral membrane glycoprotein, in polarized epithelial cells. Mol. Cell. Biol. **5:**2181–2189.
17. **Kilpatrick, D. P., R. V. Srinivas, and R. W. Compans.** 1988. Expression of the spleen focus-forming virus envelope gene in polarized epithelial cells. Virology **164:**547–550.
18. **Kristakis, N. T., D. Thomas, and M. G. Roth.** 1990. Characteristics of the tyrosine recognition signals for internalization of transmembrane surface glycoproteins. J. Cell Biol. **111:**1393–1407.
19. **Kundu, A., M. Abdul Jabbar, and D. P. Nayak.** 1991. Cell surface transport, oligomerization, and endocytosis of chimeric type II glycoproteins: role of cytoplasmic and anchor domains. Mol. Cell. Biol. **11:**2675–2685.
20. **Kundu, A., and D. P. Nayak.** 1994. Analysis of the signals for polarized transport of influenza virus (A/WSN/33) neuraminidase and human transferrin receptor, type II transmembrane proteins. J. Virol. **68:**1812–1818.
21. **Laemmli, U. K.** 1970. Cleavage of structural proteins during the assembly of the head of bacteriophage T4. Nature (London) **227:**680–685.
22. **Lazarovits, J., and M. Roth.** 1988. A single amino acid change in the cytoplasmic domain allows the influenza virus hemagglutinin to be endocytosed through coated pits. Cell **53:**743–752.
23. **Le Bivic, A., Y. Sambuy, A. Patzak, N. Patil, M. Chao, and E. Rodriguez-Boulan.** 1991. An internal deletion in the cytoplasmic tail reverses the apical localization of human NGF receptor in transfected MDCK cells. J. Cell Biol. **115:**607–618.
24. **Lisanti, M. P., I. W. Caras, M. A. Davitz, and E. Rodriguez-Boulan.** 1989. A glycophospholipid membrane anchor acts as an apical targeting signal in polarized epithelial cells. J. Cell Biol. **109:**2145–2156.
25. **Lisanti, M. P., A. Le Bivic, M. Sargiacomo, and E. Rodriguez-Boulan.** 1989. Steady state distribution and biogenesis of endogenous MDCK glycoproteins: evidence for intracellular sorting and polarization surface delivery. J. Cell Biol. **109:**2117–2128.
26. **Lisanti, M. P., M. Sargiacomo, L. Graeve, A. R. Saltiel, and E. Rodriguez-Boulan.** 1988. Polarized apical distribution of glycophosphatidylinositol-anchored proteins in a renal epithelial cell line. Proc. Natl. Acad. Sci. USA **85:**9557–9561.
27. **Lobigs, M., Z. Hongxing, and H. Garoff.** 1990. Function of Semliki Forest virus E3 peptide in virus assembly: replacement of E3 with an artificial signal peptide abolishes spike heterodimerization and surface expression of E1. J. Virol. **64:**4346–4355.
28. **Matlin, K. S.** 1986. The sorting of proteins to the plasma membrane in epithelial cells. J. Cell Biol. **103:**2565–2568.
29. **Matter, K., W. Hunziker, and I. Mellman.** 1992. Basolateral sorting of LDL receptor in MDCK cells: the cytoplasmic domain contains two tyrosine-dependent targeting determinants. Cell **71:**741–753.
30. **Matter, K., J. A. Whitney, E. M. Yamamoto, and I. Mellman.** 1993. Common signals control low density lipoprotein receptor sorting in endosomes and the Golgi complex of MDCK cells. Cell **74:**1053–1064.
31. **McQueen, N. L., D. P. Nayak, L. V. Jones, and R. W. Compans.** 1984. Chimeric influenza virus hemagglutinin containing either the NH_2-terminus

or the COOH-terminus of G protein of vesicular stomatitis virus is defective in transport to the cell surface. Proc. Natl. Acad. Sci. USA **81:**395–399.
32. **McQueen, N. L., D. P. Nayak, E. B. Stephens, and R. W. Compans.** 1986. Polarized expression of a chimeric protein in which the transmembrane and cytoplasmic domains of the influenza virus hemagglutinin have been replaced by those of the vesicular stomatitis virus G protein. Proc. Natl. Acad. Sci. USA **83:**9318–9322.
33. **McQueen, N. L., D. P. Nayak, E. B. Stephens, and R. W. Compans.** 1987. Basolateral expression of a chimeric protein in which the transmembrane and cytoplasmic domains of vesicular stomatitis virus G protein have been replaced by those of the influenza virus hemagglutinin. J. Biol. Chem. **262:** 16233–16240.
34. **Morrison, T. G., and L. J. McGinnes.** 1985. Cytochlasin D accelerates the release of Newcastle disease virus from infected cells. Virus Res. **4:**93–106.
35. **Mostov, K. E., A. de Bruyn Kops, and D. L. Deitcher.** 1986. Deletion of the cytoplasmic domain of the polymeric immunoglobulin receptor prevents basolateral localization and endocytosis. Cell **47:**359–364.
36. **Nayak, D. P., K. Tobita, J. M. Janda, A. R. Davis, and B. K. De.** 1978. Homologous interference mediated by defective interfering influenza virus derived from a temperative-sensitive mutant of influenza virus. J. Virol. **28:**375–386.
37. **Neame, S. J., and C. M. Isacke.** 1993. The cytoplasmic tail of CD44 is required for basolateral localization in epithelial MDCK cells but does not mediate association with the detergent insoluble cytoskeleton of fibroblasts. J. Cell Biol. **121:**1299–1310.
38. **Powell, S. K., B. A. Cunningham, G. M. Edelman, and E. Rodriguez-Boulan.** 1991. Targeting transmembrane and GPI-anchored forms of N-CAM to opposite domains of a polarized epithelial cell. Nature (London) **353:**76–77.
39. **Prill, V., L. Lehmann, K. von Figura, and C. Peters.** 1993. The cytoplasmic tail of lysosomal acid phosphatase contains overlapping but distinct signals for basolateral sorting and rapid internalization in polarized MDCK cells. EMBO J. **12:**2181–2193.
40. **Puddington, L., C. Woodgett, and J. K. Rose.** 1987. Replacement of the cytoplasmic domain alters sorting of a viral glycoprotein in polarized cells. Proc. Natl. Acad. Sci. USA **84:**2756–2760.
41. **Rodriguez-Boulan, E., and M. Pendergast.** 1980. Polarized distribution of viral envelope proteins in the plasma membrane of infected epithelial cells. Cell **20:**45–54.
42. **Rodriguez-Boulan, E., P. J. Salas, M. Sargiacomo, M. Lisanti, A. Le Bivic, Y. Sambuy, D. Vega-Salas, and L. Graeve.** 1989. Methods to estimate the polarized distribution of surface antigens in cultured epithelial cells. Methods Cell Biol. **32:**37–110.
43. **Rodriguez-Boulan, E. J., and D. D. Sabatini.** 1978. Asymmetric budding of viruses in epithelial monolayers: a model for the study of epithelial polarity. Proc. Natl. Acad. Sci. USA **75:**5071–5075.
44. **Roman, L. M., and H. Garoff.** 1986. Alteration of the cytoplasmic domain of the membrane spanning glycoprotein p62 of Semliki Forest virus does not affect its polar distribution in established lines of Madin-Darby canine kidney cells. J. Cell Biol. **103:**2607–2618.
45. **Roth, M. G., R. W. Compans, L. Giusti, A. R. Davis, D. P. Nayak, M. J. Gething, and J. Sambrook.** 1983. Influenza virus hemagglutinin expression is polarized in cells infected with recombinant SV 40 viruses carrying cloned hemagglutinin DNA. Cell **33:**435–443.
46. **Roth, M. G., C. Doyle, J. Sambrook, and M.-J. Gething.** 1986. Heterologous transmembrane and cytoplasmic domains direct functional chimeric influenza virus hemagglutinins into the endocytic pathway. J. Cell Biol. **102:**1271–1283.
47. **Roth, M. G., D. Gunderson, N. Patil, and E. Rodriguez-Boulan.** 1987. The large external domain is sufficient for the correct sorting of secreted or chimeric influenza virus hemagglutinin in polarized monkey kidney cells. J. Cell Biol. **104:**769–782.
48. **Roth, M. G., R. V. Srinivas, and R. W. Compans.** 1983. Basolateral maturation of retroviruses in polarized epithelial cells. J. Virol. **45:**1065–1073.
49. **Sanderson, C. M., R. Avalos, A. Kundu, and D. P. Nayak.** 1995. Interaction of Sendai viral F, HN and M proteins with host cytoskeletal and lipid components in Sendai virus-infected BHK cells. Virology **209:**701–707.
50. **Sanderson, C. M., H.-H. Wu, and D. P. Nayak.** 1994. Sendai virus M protein binds independently to either the F or the HN glycoprotein in vivo. J. Virol. **68:**69–76.
51. **Scheiffele, P., J. Peränen, and K. Simons.** 1995. N-glycans as apical sorting signals in epithelial cells. Nature (London) **378:**96–98.
52. **Simons, K., and G. van Meer.** 1988. Lipid sorting in epithelial cells. Biochemistry **27:**6197–6202.
53. **Simons, K., and A. Wandinger-Ness.** 1990. Polarized sorting in epithelia. Cell **62:**207–210.
54. **Skibbens, J. E., M. G. Roth, and K. S. Matlin.** 1989. Differential extractibility of influenza virus hemagglutinin during intracellular transport in polarized epithelial cells and nonpolar fibroblasts. J. Cell Biol. **108:**821–832.
55. **Tashiro, M., J. T. Seto, H.-D. Klenk, and R. Rott.** 1993. Possible involvement of microtubule disruption in bipolar budding of a Sendai virus mutant, F1-R, in epithelial MDCK cells. J. Virol. **67:**5902–5910.
56. **Tashiro, M., M. Yamakawa, K. Tobita, H. D. Klenk, R. Rott, and J. T. Seto.** 1990. Altered budding site of pantropic mutant of Sendai virus, F1-R, in polarized epithelial cells. J. Virol. **64:**4672–4677.
57. **Thomas, D. C., C. B. Brewer, and M. G. Roth.** 1993. Vesicular stomatitis virus glycoprotein contains a dominant cytoplasmic basolateral sorting signal critically dependent upon a tyrosine. J. Biol. Chem. **268:**3313–3320.
58. **Thomas, D. C., and M. G. Roth.** 1994. The basolateral targeting signal in the cytoplasmic domain of glycoprotein G from vesicular stomatitis virus resembles a variety of intracellular targeting motifs related by primary sequence but having diverse targeting activities. J. Biol. Chem. **269:**15732–15739.
59. **vanMeer, G., and K. Simons.** 1982. Viruses budding from either the apical or the basolateral plasma membrane domain of MDCK cells have unique phospholipid compositions. EMBO J. **1:**847–852.
60. **Vogel, L. K., O. Noren, and H. Sjostrom.** 1995. Transcytosis of aminopeptidase N in Caco-2 cells is mediated by a non-cytoplasmic signal. J. Biol. Chem. **270:**22933–22938.
61. **Yokode, M., R. K. Pathak, R. E. Hammer, M. S. Brown, J. L. Goldstein, and R. G. W. Anderson.** 1992. Cytoplasmic sequence required for basolateral targeting of LDL receptor in livers of transgenic mice. J. Cell Biol. **117:**39–46.
62. **Zurzolo, C., W. van't Hof, G. van Meer, and E. Rodriguez-Boulan.** 1994. VIP21/caveolin, glycosphingolipid clusters and the sorting of glycosylphosphatidylinositol-anchored proteins in epithelial cells. EMBO J. **13:**42–53.